Appl. Phys. B 86, 677–680 (2007)
DOI: 10.1007/s00340-006-2525-2

Applied Physics B
Lasers and Optics

X.-Z. ZHANG
D.-M. ZHANG✉
S.-K. MU
D. ZHANG
C. CHEN

1.53 μm photoluminescence from ErYb(DBM)$_3$MA containing polymer

National Integrated Optoelectronics Laboratory, College of Electronic Science and Engineering, Jilin University, Qianjin Street 2699, Changchun 130012, China

Received: 1 August 2006/Revised version: 2 October 2006
Published online: 12 December 2006 •

ABSTRACT We investigated the optical properties of the ErYb(DBM)$_3$MA complexes and the ErYb(DBM)$_3$MA containing polymer. Absorption and photoluminescence spectra confirm that the presence of Yb^{3+} ions enhances luminescence efficiency of Er^{3+} ions. The full width at half maximum bandwidth (FWHM) is ∼ 80 nm wide around 1.53 μm wavelength. We also fabricated ErYb containing polymeric channel waveguides using reactive ion etching technique. As an input pump of 120 mW was used, a ∼ 1.53 μm spontaneous emission was obtained in a 4-mm-long waveguide.

PACS 42.00.00; 42.70.Jk; 42.82.Et

1 Introduction

Planar optical waveguide devices and circuits are essential for optical fiber communication systems, especially in the metropolitan area networks and the local area networks. In order to compensate optical losses and provide efficient light transmission, optical amplifiers are indispensable. Erbium-doped waveguide amplifiers (EDWA) have been demonstrated in glass hosts [1–6].

Polymeric optical waveguide devices have many advantages because of their low costs, high packaging density, and simple processing steps. Various techniques such as photobleaching [7, 8], ion-implantation [9], direct write electron beam [10–12], and reactive ion beam etching (RIE) [13] have been used to fabricate polymeric channel waveguide. Using RIE technique, we can avoid some destroying processes in other techniques that may degrade the optical activity of the core material [14]. In addition, the RIE is compatible with conventional semiconductor process. It is possible to fabricate an erbium-doped active waveguide by using polymer as host material. As a polymer material, particular interest in PMMA-based polymer arises from its low cost, refractive index tailorability with molecular weight, good optical transparency and resistance to laser damage. These characteristics make it suitable as a host material for rare-earth ions [15, 16]. The optical amplification of Eu(DBM)$_3$phen-doped polymer optical fiber was demonstrated by using a PMMA host [17].

✉ Fax: 86-431-5168270, E-mail: zhangdm@mail.jlu.edu.cn

Compared to inorganic host materials, it is relatively difficult to dissolve rare earth ions in polymers, because most of the rare earth ions are inorganic salt forms. Inorganic salts do not mix well with polymers and coagulation occurs. In the past years, multifarious organic rare-earth complexes have been synthesized and characterized. Some rare earth complexes can be blended into polymer solution [12, 18, 19]. But other rare earth complexes are poorly soluble in the polymer solution. To settle this problem, we covalently incorporate the rare-earth complex into polymer hosts up to higher concentration. In this way, we reduce the influence of the concentration quenching on the photoluminescence (PL) intensity.

Our objective is to investigate 980 nm laser diode pumped amplifier which is compatible with current components in the fiber communication. Direct excitation of Er^{3+} ions in organic complexes at 980 nm wavelength has lower pump efficiency due to a small absorption cross section. There are two approaches to enhance absorption cross section of active material and luminescence intensity. The first approach utilizes ligand absorption and intersystem crossing mechanism. Slooff et al. have reported the Er^{3+}-doped organic cage-like complexes and the complex-doped polymeric waveguide [18]. The ligand absorption cross section is 8.5×10^{-18} cm^2 at 287 nm, much higher than 1.1×10^{-20} cm^2 (the cross section for direct absorption of the Er^{3+} ion at 488 nm). According to rate equations, the 0 dB gain threshold pump power of a 2 μm × 1 μm active waveguide could be decreased from 930 to 1.4 mW. A challenge in their work is to engineer the ligand and to shift the excitation wavelength in order to use semiconductor lasers as pump lasers. And H. Wang et al. reported an ion-association ternary complex Er(HFA)$_4$IR5 [19]. The IR5 segment was used as a sensitizer to enhance absorption intensity around 980 nm and the PL intensity at 1.53 μm. The second approach is based on energy transfer from other rare ions to Er^{3+} ions. The Yb^{3+} ion is normally used as the sensitizer due to large absorption cross section at 980 nm. An efficient energy transfer from Yb^{3+} to Er^{3+}ions have been reported by using Er^{3+}-Yb^{3+} organic pentanedione derivatives in epoxy novolac resin (ENR) [8, 12]. Up to now, for the Er^{3+}-doped polymer amplifiers, only W.H. Wong et al. demonstrated experimental internal gains of 13 dB and 16.5 dB using this ENR.

In this letter, we report on a new Er-Yb containing polymeric optical waveguide material. The absorption, the PL spectra and the impact of the doping concentration on PL

spectra were investigated. Furthermore, we observed spontaneous emission in a 4-mm-long channel waveguide.

2 Experiments and results

The cladding material is poly-methyl-methacrylate-co-glyciclyl-methacrylate P(MMA-co-GMA), and the core material is the mixture of P(MMA-co-GMA) and bis-phenol-A epoxy. The refractive index of the core material at 1.53 μm is subject to precise control in the range of 1.480 to 1.580. In order to introduce active medium, the organic complex $Er(DBM)_3MA$ and $ErYb(DBM)_3MA$ were synthesized and covalently incorporated to core polymer main chain to form the active ErYb containing core material.

Absorption spectra of the complex powder were determined from reflection measurements using a spectrometer and an integrating sphere (spectral resolution 1 nm), and are shown in Fig. 1a. The complexes powder samples S1 ($Er(DBM)_3MA$ powder) and S2 ($ErYb(DBM)_3MA$ powder) were prepared in $BaSO_4$ powder. The weight concentrations of Er ions are equal in S1 and S2. As is shown in Fig. 1a, the absorption intensity at 1.5 μm is almost the same in the two samples, but a $\sim 1/3$ absorption enhancement at 976 nm peak in S2 is observed and ascribed to Yb ions absorption. The corresponding transitions are ${}^4I_{15/2} - {}^4I_{11/2}$ (Er^{3+}) in S1 and ${}^4I_{15/2} - {}^4I_{11/2}$ (Er^{3+}) ${}^2F_{7/2} - {}^2F_{5/2}$($Yb^{3+}$) in S2. The level notation is specified at corresponding transition peak. The absorbance spectra of the $ErYb(DBM)_3MA$ containing polymer solution S3 and polymer tablet S4 were determined from transmission measurements, and are shown in Fig. 1b and c, respectively. In the case of Fig. 1b, the $ErYb(DBM)_3MA$ containing polymer solution of the butyl acetate (need adjust to appropriate concentration) are prepared in a 1 cm standard quartz cell. Another quartz cell of butyl acetate was used as the reference. In the case of Fig. 1c, above ErYb polymer solution was solidified in a model and the bulk polymer was cut to form a polymer tablet in 0.4 mm thickness. In both Fig. 1b and c, the steadily increasing background in the wavelength range down to ∼800 nm is mainly attributed to scattering in polymer solution and tablet [18]. In the near-infrared region of Fig. 1, relatively strong absorption bands in polymer material are located around 1.1–1.2 μm, 1.35–1.45 μm and above 1.6 μm due to the vibrational overtones of O–H and C–H vibrations [15, 18].

The PL spectra of Er^{3+} and Er^{3+}-Yb^{3+}containing polymer were investigated using standard lock-in technique. A laser diode operating at 976 nm and a liquid nitrogen cooled Ge photodiode were used as excited source and detector, respectively. An Er^{3+} and Er^{3+}-Yb^{3+}containing polymer was prepared on Si wafer and solidified at 120 °C for 3 h. Figure 2 shows the PL spectra of $ErYb(DBM)_3MA$ containing polymers with different Er ions concentration (Er^{3+}:Yb^{3+} = 1 : 3 in weight). The fluorescence peak at 1530 nm is associated with ${}^4I_{13/2} - {}^4I_{15/2}$ transition. As the concentration of Er ions increases, the peak PL intensity gradually increases. The full width at half maximum is ∼ 80 nm, which is the largest value in Er ions containing system. As we know, the FWHM values are ∼30–45 nm in ErYb-co-doped phosphate glasses [1, 2], ∼70 nm in Er^{3+}-doped organic polydentate cage complexes [18]. The shoulders in PL spectra are attributed to transitions from the lowest Stark level in first excited state ${}^4I_{13/2}$ to the eight Stark splitting levels in ground state ${}^4I_{15/2}$ [20].

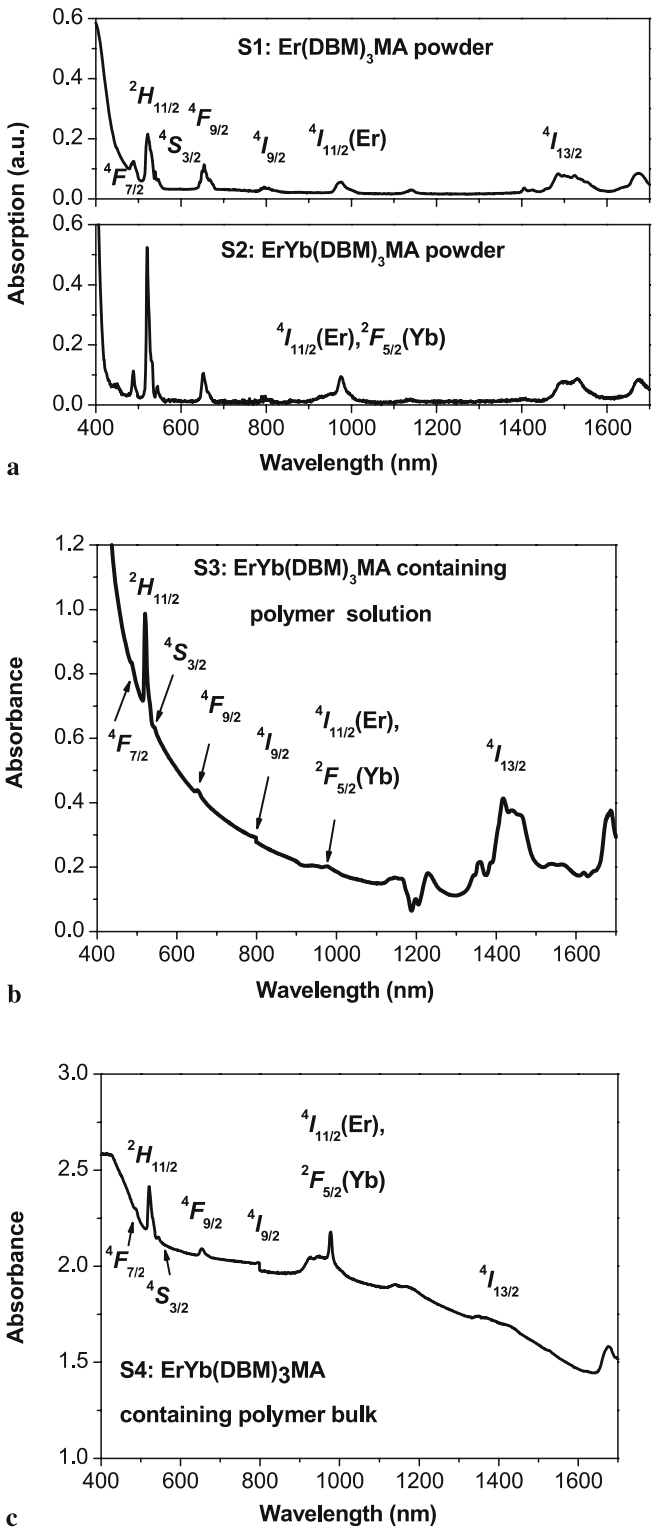

FIGURE 1 (**a**): Absorption spectra of $Er(DBM)_3MA$ (S1) and $ErYb(DBM)_3MA$ powder (S2). (**b**): Absorbance of $ErYb(DBM)_3MA$ containing polymer solution (S3). (**c**): Absorbance of $ErYb(DBM)_3MA$ containing polymer tablet in 0.4 mm thickness (S4)

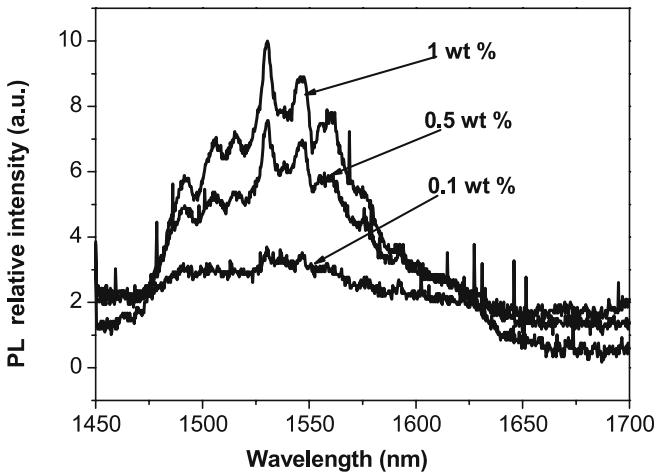

FIGURE 2 PL spectra of ErYb(DBM)$_3$MA containing polymer with different concentrations of Er^{3+} ions (Er^{3+}:Yb^{3+} = 1 : 3 in weight). The excitation wavelength was 976 nm at a pump power of 60 mW

Figure 3 shows the dependence of PL intensity at the peak (∼1530 nm) on Yb ions concentration in ErYb(DBM)$_3$MA containing polymer. The concentration of Yb^{3+} ions varied from 0 to 8 wt. % and concentration of Er^{3+} ions were kept at 1 wt. %. From Fig. 3, a suitable concentration of Yb^{3+} ions was about 3 wt. %. Compared the maximum with the minimum, the PL intensity is enhanced by a factor 5 due to energy transfer from $Yb^{3+}$to Er^{3+} ions. The explanation for a decrease of the peak PL intensity at high Yb concentrations is that some up conversion mechanism in Yb ions becomes more and more competitive with the Yb-to-Er energy transfer mechanism, thus reducing the pumping efficiency and consequently the intensity of the fluorescence spectrum.

For preparation of the active waveguide, thermally oxidized silicon wafers with ∼2.2-μm-thick oxide layer were used as substrates, and the oxide layer acts as the lower cladding layer. The ErYb containing polymer (Er 1 wt. %, Yb 3 wt. %) was spun on top as the waveguide core layer and baked at 120 °C to remove the solvent. Then the aluminum film with the thickness of 10–30 nm was vaporized on the surface of the core layer. The device mask was patterned by photolithography. The core ridge was formed by RIE using oxygen. After the masks were removed, the core ridge was covered with an over-cladding layer P(MMA-co-GMA) by spin coating. Finally, the channel waveguides embedded on a Si wafer were cut to the required length. Three layers of film were characterized optically by the M-2000UI variable angle incidence spectroscopic ellipsometer. At 1530 nm wavelength, the refractive indexes are 1.456 (lower cladding), 1.505 (core layer) and 1.480 (over cladding), respectively. Figure 4 shows the titled SEM image of a 6 μm × 4 μm ErYb containing active polymeric waveguide (no over-cladding layer).

The forward pump gain measurement configuration was used. A tunable laser operating at 1510–1590 nm was used as signal source, and a 976 nm laser diode was used as pump source. Both pump and signal laser were coupled by a 980/1550 nm wavelength divide multiplexer and together butt-coupled to the active waveguide. An optical spectrum analyzer was used to record output spectra. The insertion loss of the waveguide comprises the Fresnel loss, the coupling loss (mode mismatch loss), the scattering loss at waveguide facet, and the propagation loss. The insertion loss of waveguide was measured in different length. We roughly estimated the Fresnel loss, the coupling loss and scattering loss at waveguide facet together ∼ 4.0 dB/facet, the propagation loss ∼ 4.0 dB/cm at 1.5 μm region in use of a cut back method. Considering the difference of the refractive indexes between the fiber and the air, we calculate the Fresnel losses at about 4% (0.18 dB) at the fiber–air interface. Considering also the waveguide–air interface (accounting for another 4% loss), we estimate roughly the fiber-to-waveguide Fresnel coupling loss to be about 0.35 dB/ facet. In order to estimate the mode mismatch loss, we measured the near field patterns (the inset in Fig. 4) of the fiber and the waveguide using an infrared CCD. The mode mismatch loss was estimated as ∼ 1.64 dB/facet using a formula in [22]. Thus the scattering loss is ∼ 2.0 dB per facet. The ∼4.0 dB/cm propagation loss consists of Er absorption, the polymer absorption, and scattering at the interface and inside the waveguide. The waveguide loss does not

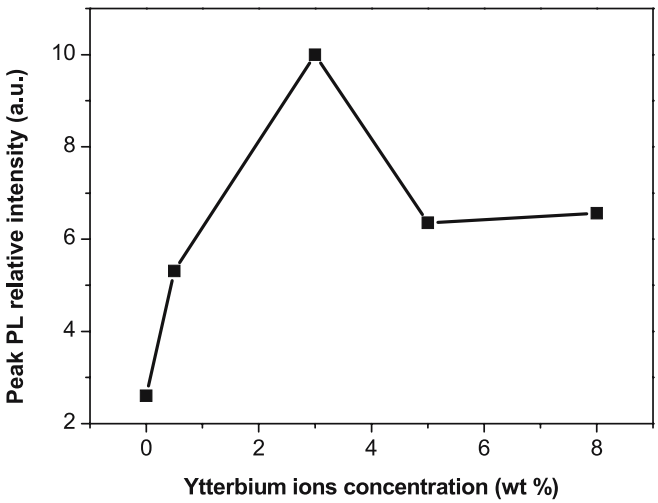

FIGURE 3 Dependence of PL intensity at peak (∼ 1530 nm) on Yb ions concentration in ErYb(DBM)$_3$MA containing polymer. The concentration of $Er^{3+}$was kept at 1 wt. %. The excitation wavelength was 976 nm at a pump power of 60 mW

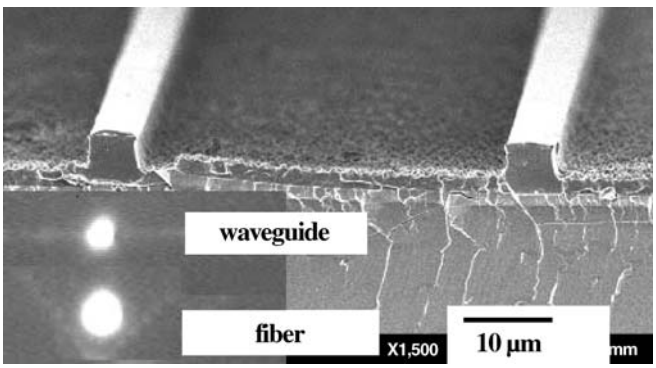

FIGURE 4 Tilted SEM image of a 6 μm×4 μm Er^{3+}-Yb^{3+} containing active waveguide using RIE technique (no over cladding layer). The *inset* is the near field pattern of the fiber and a 4-mm-long waveguide at input power -20 dBm and wavelength 1530 nm

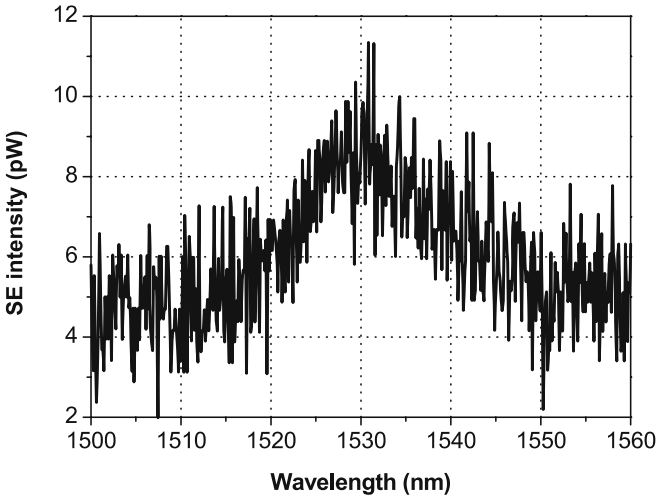

FIGURE 5 The spontaneous emission (SE) spectrum from a 4-mm-long waveguide. The spectral resolution is 1 nm. The excitation wavelength was 976 nm at a pump power of 120 mW

increase near the 1.5 μm region (due to the absorption of the Er ions), indicating that Er absorption loss is not a main source and the intrinsic waveguide propagation loss is too high. The propagation loss mainly comes from the waveguide scattering and polymer absorption. A spontaneous emission (SE) spectrum with peak value of ∼ 10 pW (spectral resolution 1 nm) was measured in 4-mm-long waveguide at a pump power of 120 mW, and was shown in Fig. 5. For more than 10-mm-long waveguide, we could not obtain spontaneous emission even pump power up to 160 mW. The relative gain (or signal enhancement from an unpumped to a pumped state) could not been obtained in all of fabricated waveguides.

3 Discussion

Let us discuss the reason why we can not get relative gain: (1) The absorption mainly comes from polymer part instead of Er ions in both 976 nm and 1530 nm region, which does not contribute to Er ions absorption and luminescence. Therefore, the luminescence efficiency is still lower by 976 nm laser pump and population inversion does not achieve. We also carried out some PL measurements to confirm this standpoint: (a) In this ErYb-containing polymer, the 1.53-μm-PL intensity by 532 nm laser pump is 1 order of magnitude stronger than that by 976 nm laser pump under same condition. (b) The 1.53-μm-PL intensity from commercial ErYb phosphate glass is ∼ 3 orders of magnitude stronger than that from ErYb-containing polymer by 976 nm laser pump. (2) The quenching mechanism from C–H and O–H groups affect the pump efficiency and the luminescence intensity [18]. The C–D or C–F bonds instead of C–H bonds can reduce the polymer quenching effect in the 1530 nm region, which is also our next orientation.

4 Conclusion

In conclusion, a suitable concentration of Yb^{3+} ions can enhance the luminescence efficiency of Er^{3+} ions. This covalent ErYb containing polymeric channel waveguides can be fabricated by photolithography and RIE technique. We can obtain spontaneous emission spectrum in a 4-mm-long waveguide. If the luminescence efficiency of this ErYb-containing polymer is improved, it is possible to be applied in EDWA.

ACKNOWLEDGEMENTS The work was supported by National Natural Science Foundation of China (Project No. 60507004) and Program for New Century Excellent Talents in University.

REFERENCES

1 S.F. Wong, E.Y.B. Pun, P.S. Chun, IEEE Photon. Technol. Lett. **14**, 80 (2002)
2 K. Liu, E.Y.B. Pun, Appl. Opt. **43**, 3179 (2004)
3 K. Liu, E.Y.B. Pun, T.C. Sum, A.A. Bettiol, J.A. van Kan, F. Watt, Appl. Phys. Lett. **84**, 684 (2004)
4 G. Della Valle, R. Osellame, N. Chiodo, S. Tacchco, G. Cerullo, P. Laporta, Opt. Express **13**, 5976 (2005)
5 R.R. Thomson, S. Campbell, I.J. Blewett, A.K. Kar, D.T. Reid, Appl. Phys. Lett. **87**, 121 102 (2005)
6 H.S. Han, S.Y. Seo, J.H. Shin, Appl. Phys. Lett. **79**, 4568 (2001)
7 Y. Shi, W.H. Steier, L. Yu, M. Chen, L.R. Dalton, Appl. Phys. Lett. **58**, 1131 (1991)
8 W.H. Wong, K.S. Chan, E.Y.B. Pun, Appl. Phys. Lett. **87**, 011 103 (2005)
9 J.R. Kulisch, H. Franke, R. Irmscher, C. Buchanl, J. Appl. Phys. **71**, 3123 (1992)
10 W.H. Wong, E.Y.B. Pun, Appl. Phys. Lett. **79**, 3576 (2001)
11 W.H. Wong, J. Zhou, E.Y.B. Pun, Appl. Phys. Lett. **78**, 2110 (2001)
12 W.H. Wong, E.Y.B. Pun, K.S. Chan, Appl. Phys. Lett. **84**, 176 (2004)
13 M. Hikita, Y. Shuto, M. Amano, R. Yoshimura, S. Tomaru, H. Kozawaguchi, Appl. Phys. Lett. **63**, 1161 (1993)
14 W. Wang, D. Chen, H.R. Fetterman, Y. Shi, W.H. Steier, L.R. Dalton, Appl. Phys. Lett. **65**, 929 (1994)
15 H. Liang, Z. Zheng, B. Chen, Q. Zhang, H. Ming, Mater. Chem. Phys. **86**, 430 (2004)
16 Z. Zheng, H. Liang, H. Ming, Q. Zhang, J. Xie, Opt. Commun. **233**, 149 (2004)
17 H. Liang, Q. Zhang, Z. Zheng, H. Ming, Z. Li, J. Xu, B. Chen, H. Zhao, Opt. Lett. **29**, 477 (2004)
18 A. Van Blaaderen, A. Polman, G.A. Hebbink, S.I. Klink, F.C.J.M.V. Veggel, D.N. Reinhoudt, J.W. Hofstraat, J. Appl. Phys. **91**, 3955 (2002)
19 H. Wang, G. Qian, M. Wang, J. Zhang, Y. Luo, J. Phys. Chem. B **108**, 8084 (2004)
20 S.F. Li, Q.Y. Zhang, Y.P. Lee, J. Appl. Phys. **96**, 4746 (2004)
21 C. Strohhöfer, A. Polman, J. Appl. Phys. **90**, 4314 (2001)
22 W.K. Burns, G.B. Hocker, Appl. Opt. **16**, 2048 (1977)